THE JOURNAL OF PHYSICAL CHEMISTRY LETTERS
A JOURNAL OF THE AMERICAN CHEMICAL SOCIETY

pubs.acs.org/JPCL

Letter

Molecular Mechanisms of Active Transport in Antiporters: Kinetic Constraints and Efficiency

Alex Berlaga and Anatoly B. Kolomeisky*

Cite This: *J. Phys. Chem. Lett.* 2021, 12, 9588–9594

Read Online

ACCESS | Metrics & More | Article Recommendations

ABSTRACT: A vital role in supporting successful functioning of biological cells is played by membrane channels called antiporters. These channel proteins utilize the concentration gradient of one type of species to move another type of species in the opposite direction and against their concentration gradient. It is believed that antiporters operate via alternating conformational transitions that expose these proteins to different sides of the membrane, and that only thermodynamics controls the activation of these channels. Here we explicitly investigate a chemical-kinetic model of antiporters to argue that there are additional kinetic constraints that need to be satisfied for these channels to be operational. This implies that kinetics and not thermodynamics governs the functioning of antiporters. In addition, the efficiency of antiporters is analyzed and the most optimal operating conditions are discussed. Our theoretical analysis clarifies some important aspects of the molecular mechanisms of biological membrane transport.

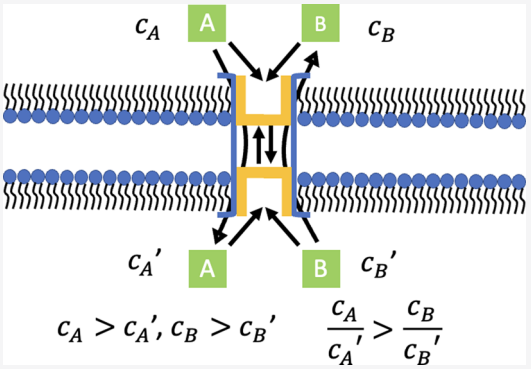

Biological cells are complex dynamic systems that constantly require the transportation of various species across the cellular membranes for their long-term survival.[1,2] For example, necessary nutrients should be moved into the cell, while waste products must be promptly removed out of the cell.[1−7] There are several classes of protein membrane channels, generally called transporters, that are devoted to these tasks.[1,2,6−8] It is often necessary to move species across the membranes against the already established gradients of their concentrations, and this clearly requires the input of energy. Nature came out with a very elegant solution of this problem: multiple classes of membrane channels use the transport of one kind of molecule along its own concentration gradient to drive the motion of another kind of molecule against its concentration gradient. This category of membrane translocations is called secondary active transport or cotransport.[1,2,6,9]

Depending on the direction of motion for both translocated species, these membrane transporters are divided into two large classes. Those where particles of both species move in the same direction are labeled as symporters,[10−12] while those where the transport of both species is happening in the opposite direction are labeled as antiporters.[3,13,14] These membrane channels have been studied using a variety of biochemical and biophysical methods.[3] However, the molecular mechanisms of their process still remain not fully understood.[6,8,15,16] In this Letter, we would like to concentrate on the microscopic origins of secondary active transport in antiporters.

Analysis of multiple experimental investigations of antiporters led researchers to suggest that these protein channels follow so-called alternating-access mechanisms.[3,7,8,15,17] According to this picture, the antiporter alternates between the protein conformations open to the outside or to the inside of the cell, and only a single substrate can bind to the channel at any time. Without a substrate bound to the antiporter, the conformational dynamics is assumed to be slow, but the association of any type of translocated species to the protein channel catalytically accelerates the conformational transitions. Although some aspects of the proposed mechanism have been supported by structural and kinetic measurements,[3,8,18,19] several open fundamental questions about the mechanism of cotransport in antiporters remain unanswered.

First, it is widely believed that mostly thermodynamic constraints govern the conditions for the activation of antiporters.[1−3] In other words, the membrane channel will always operate if the concentration gradient of the driving species is larger than the concentration gradient of the driven species. But such conclusions about the tight-coupling mechanism of cotransport are frequently obtained by analyzing

Received: August 30, 2021
Accepted: September 24, 2021
Published: September 28, 2021

thermodynamically inconsistent chemical-kinetic models where some transitions are arbitrarily assumed to be irreversible and transitions between other states are neglected.[3,15] It is not clear, however, whether properly considering all chemical transitions that are occurring in cotransport would always lead to the tight-coupling picture. At the same time, it should be noted that in his classical book Terrell Hill already considered the possibility of deviation from the tight-coupling picture due to so-called "leakage" processes, but the analysis presented there is mostly phenomenological and it discusses only symporters with multisite occupation.[20] A second surprising observation is that for some processes of transporting the same compounds across a membrane, there exists a large variety of structurally different antiporters.[3,21] If the antiporters would follow a tight-coupling mechanism, then one would expect to have only one or a few types of channels for each substrate in the given cellular environment. These observations suggest that the understanding of the molecular mechanisms of antiporters is far from complete.

In this Letter, we hypothesize that thermodynamics does not always determine the activation conditions of the antiporters and that there are additional kinetic constraints that should be also considered. To test this idea, we explicitly investigate a minimal chemical-kinetic model of the antiporters that properly accounts for chemical transitions in the system. It is found that for some ranges of parameters, the antiporter does not operate even if the thermodynamic conditions are satisfied. The analysis suggests how the specific transitions might optimize the flux of the driven species in the system. Our theoretical approach naturally explains the existence of a large number of apparently redundant membrane channels. Thus, the proposed theoretical framework clarifies some aspects of the molecular mechanisms of cotransport in antiporters.

Let us consider a minimal chemical-kinetic model of secondary active transport as presented in Figure 1. This

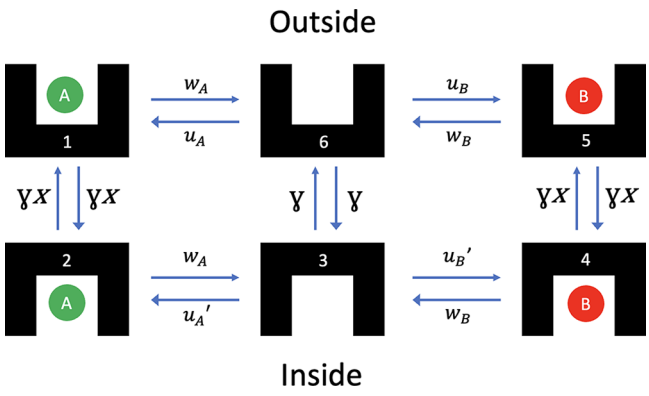

Figure 1. Minimal chemical-kinetic model of antiporter activities that follows the rocking-bundle mechanism. Upper three states correspond to the protein conformations opened to the outside of the cell, while three lower states correspond to protein conformations exposed to the inside medium of the cell. More details of the model are explained in the text.

model follows the widely accepted alternating-access mechanism for antiporters.[3,8,15,22,23] There are six distinct chemical states in the system. Three of them (states 1, 6, and 5) describe the situations when the membrane channel is opened to the outside of the cell, and three other states (states 2, 3, and 4) correspond to protein conformations opened to the inside of the cell: see Figure 1. There are two types of substrates, labeled as A and B, that participate in the membrane transport. The concentrations of substrates A and B above the channel are equal to c_A and c_B, respectively. The concentrations below the channel are assumed to be c_A' and c_B', respectively. There are more species of both types outside of the membrane, that is, $c_A > c_A'$ and $c_B > c_B'$. We assume that the antiporter operates when the particles of type A drive the motion of the particles of type B. In the situation shown in Figure 1, the molecules A move downward along their gradient forcing the molecules B to move upward against their gradient.

In our model, if the transporter is facing up, the particle A (B) can bind to the protein channel with a rate $u_A = kc_A$ ($u_B = kc_B$). This means that we assume the same association rate constants k for both molecules of type A and B. These associations correspond to transitions between the states 6 → 1 and 6 → 5: see Figure 1. But the species A and B might also dissociate back into the solution with transition rates w_A and w_B, respectively. These dissociations correspond to transitions between the states 1 → 6 and 5 → 6: see Figure 1. Similarly, when the channel is facing down, the associations of substrates A and B with the transporter are taking place with rates $u_A' = kc_A'$ and $u_B' = kc_B'$ (transitions 3 → 2 and 3 → 4 in Figure 1, respectively). The reverse unbinding transitions of species A and B (transitions 2 → 3 and 4 → 3 in Figure 1) are happening with rates w_A' and w_B', respectively.

In this Letter, we also assume that $w_A = w_A'$ and $w_B = w_B'$. This is due to the fact that conformations of the channel protein are the same and only differ by inversion: they are faced up or down. Then the dissociation rates are determined by the channel−substrate intermolecular interactions that seem to be very similar in these cases. In addition, we checked using Monte Carlo simulations that for the situations when $w_A \neq w_A'$ there are little deviations from our results, justifying the approximation $w_A = w_A'$.

The important part of the rocking-bundle mechanism is the ability of the protein channel to change its conformations between opening up and opening down. In our model, such conformational transitions (6 ↔ 3 in Figure 1) are taking place with a rate γ if the transporter is empty. However, the conformational transition rates between the occupied channel states (1 ↔ 2 and 5 ↔ 4 in Figure 1) are occurring with rates $x\gamma$. The dimensionless parameter x reflects the ability of substrates A and B to modify the conformational transition rates. For simplicity, we assume here that both species have the same effect on conformational transition barriers. In addition, $x > 1$ corresponds to the catalytic effects when the conformational transitions rates are accelerated, while $x < 1$ describes the inhibition effect when the conformational transitions rates are slowed down. Thus, in our model we assume that binding of substrates to the transporter modifies only the transition state energies of conformational processes without modifying the free energy differences for the channels facing up or down.

To understand the dynamics of molecular processes in antiporters, we introduce functions $P_i(t)$ ($i = 1, ..., 6$) that are defined as the probability to find the system in state i at time t. The temporal evolution of these probabilities is governed by a set of master equations,

https://doi.org/10.1021/acs.jpclett.1c02846
J. Phys. Chem. Lett. 2021, 12, 9588−9594

$$\begin{cases} \frac{dP_1(t)}{dt} = -(\gamma x + w_A)P_1(t) + \gamma x P_2(t) + u_A P_6(t) \\ \frac{dP_2(t)}{dt} = \gamma x P_1(t) - (\gamma x + w_A)P_2(t) + u_A' P_3(t) \\ \frac{dP_3(t)}{dt} = w_A P_2(t) - (\gamma + u_A' + u_B')P_3(t) + w_B P_4(t) + \gamma P_6(t) \\ \frac{dP_4(t)}{dt} = u_B' P_3(t) - (\gamma x + w_B)P_4(t) + \gamma x P_5(t) \\ \frac{dP_5(t)}{dt} = \gamma x P_4(t) - (w_B + \gamma x)P_5(t) + u_B P_6(t) \\ \frac{dP_6(t)}{dt} = w_A P_1(t) + \gamma P_3(t) + w_B P_5(t) - (\gamma + u_A + u_B)P_6(t) \end{cases} \quad (1)$$

They are also supplemented with the normalization condition, $P_1(t) + P_2(t) + P_3(t) + P_4(t) + P_5(t) + P_6(t) = 1$. We are interested in the stationary behavior of the system ($t \to \infty$) when the master equations can be explicitly solved, yielding the steady-state probabilities of different states of the antiporter,

$$\begin{aligned} P_1 &= \frac{w_B}{N}[u_A w_A(w_B + 2\gamma x + u_B' x) + \gamma x(u_A + u_A')(2\gamma x + w_B) \\ &\quad + u_A u_A' x(w_B + 2\gamma x) + \gamma x^2(u_A u_B' + u_B u_A')] \\ P_2 &= \frac{w_B}{N}[u_A' w_A(w_B + 2\gamma x + u_B x) + \gamma x(u_A + u_A')(2\gamma x + w_B) \\ &\quad + u_A u_A' x(w_B + 2\gamma x) + \gamma x^2(u_A u_B' + u_B u_A')] \\ P_3 &= \frac{w_A w_B}{N}[w_B u_A x + w_A u_B x + 2\gamma x(u_A + u_B + w_A + w_B + 2\gamma x) \\ &\quad + w_A w_B] \\ P_4 &= \frac{w_A}{N}[u_B' w_B(w_A + 2\gamma x + u_A x) + \gamma x(u_B + u_B')(2\gamma x + w_A) \\ &\quad + u_B u_B' x(w_A + 2\gamma x) + \gamma x^2(u_A u_B' + u_B u_A')] \\ P_5 &= \frac{w_A}{N}[u_B w_B(w_A + 2\gamma x + u_A' x) + \gamma x(u_B + u_B')(2\gamma x + w_A) \\ &\quad + u_B u_B' x(w_A + 2\gamma x) + \gamma x^2(u_A u_B' + u_B u_A')] \\ P_6 &= \frac{w_A w_B}{N}[w_B u_A' x + w_A u_B' x + 2\gamma x(u_A' + u_B' + w_A + w_B \\ &\quad + 2\gamma x) + w_A w_B] \end{aligned} \quad (2)$$

In these expressions, the coefficient N is a normalizing parameter given by

$$\begin{aligned} N &= w_B(w_B + 2\gamma x)[2u_A(\gamma + u_A')x + u_A w_A(1 + x) \\ &\quad + 2w_A(w_A + 2\gamma x) + u_A'(w_A + 2\gamma x + w_A x)] + u_B' \\ &\quad [2\gamma u_A w_B x^2 + w_A^2(w_B + 2\gamma x + w_B x) \\ &\quad + 2w_A x(u_A w_B + 2\gamma^2 x + \gamma(w_B(1 + x) + u_A x)] \\ &\quad + u_B[2\gamma u_A' w_B x^2 + w_A^2(2\gamma x + 2u_B' x + w_B(1 + x)) \\ &\quad + 2w_A x(u_A' w_B + 2\gamma^2 x + \gamma(w_B + (u_A' + 2u_B' + w_B)x))] \end{aligned} \quad (3)$$

Knowing the steady-state probabilities for different chemical states allows us to fully evaluate the stationary dynamics of the antiporter. The flux of particles A, J_A, is considered to be positive if they move from the outside to the inside regions (Figure 1). The flux of particles B, J_B, is viewed as positive when it occurs from the inside to the outside regions (Figure 1). The stationary particle current of the species B can be evaluated as

$$\begin{aligned} J_B &= \gamma x(P_4 - P_5) \\ &= \frac{\gamma x w_A w_B}{N}[u_B'(w_A + 2\gamma x + u_A x) - u_B(w_A + 2\gamma x + u_A' \\ &\quad x)] \end{aligned} \quad (4)$$

The antiporter is operational when $J_B > 0$, that is, when the particles B move against their gradient, which from eq 4 leads to the following kinetic condition of the cotransport:

$$u_B'(w_A + 2\gamma x + u_A x) > u_B(w_A + 2\gamma x + u_A' x) \quad (5)$$

It can be rewritten as

$$\frac{g_A}{g_B} > \frac{1 + \frac{2\gamma}{u_A'} + \frac{w_A}{x u_A'}}{1 + \frac{2\gamma}{u_A} + \frac{w_A}{x u_A}} \quad (6)$$

where new parameters are defined as $g_A = u_A/u_A' = c_A/c_A'$ and $g_B = u_B/u_B' = c_B/c_B'$. The physical meaning of these parameters is the following. The quantities g_A and g_B can be viewed as dimensionless measures of the thermodynamic forces that tend to move the molecules from the region with higher concentration to the region with lower concentration. One could also notice that $k_B T \ln g_A = k_B T \ln(c_A/c_A')$ and $k_B T \ln g_B = k_B T \ln(c_B/c_B')$ give free energy differences for the molecules A and B, respectively, to be found between the outside and the inside regions of the cellular membrane (see Figure 1). This is because the chemical potentials for molecules A to be found above and below the membrane are proportional to $k_B T \ln c_A$ and $k_B T \ln c_A'$, respectively. There are similar expressions for species B. Then the thermodynamic condition of the cotransport can be written as $g_A > g_B$ or simply as $g_A/g_B > 1$. In other words, the free energy due to the gradient of molecules A must be larger than the energy due to the gradient of molecules B for the transport to be possible, $k_B T \ln g_A > k_B T \ln g_B$.

Since $u_A/u_A' > 1$, from eq 6, it can be concluded that the kinetic conditions on the existence of secondary active transport in antiporters are always more strict than the thermodynamic conditions. This can be also clearly seen in Figure 2 where both types of conditions are plotted together. The parameter space where the secondary active transport might happen according to kinetic criteria is shown as the blue shaded region below the solid lines, while the thermodynamic condition suggests the region below the dashed line; see Figure 2. Importantly, there is always a region (between the dashed

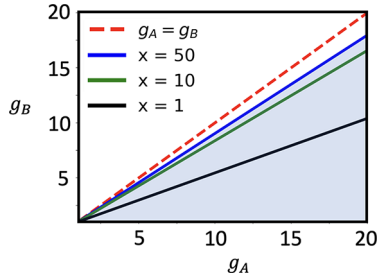

Figure 2. Comparison of thermodynamic and kinetic conditions of cotransport in the antiporters. Red dashed line describes the thermodynamic boundary, while solid lines correspond to kinetic boundaries for different values of the catalytic parameter x. The following parameters were used in calculations: $\gamma = 1\ s^{-1}$, $w_A = 100\ s^{-1}$, and $u_A' = 100\ s^{-1}$.

https://doi.org/10.1021/acs.jpclett.1c02846
J. Phys. Chem. Lett. 2021, 12, 9588−9594

and solid lines) where the thermodynamic force due to the gradient of species A is larger than the thermodynamic force due to the gradient of species B, but particles B still move along their gradient. For any fixed value of g_B, an additional gradient in molecules A (in comparison with thermodynamic arguments) is required to make the antiporter operational. One can also see in Figure 2 the importance of the catalytic effect on accelerating the conformation dynamics due to binding of substrates to the channel. Larger values of the catalytic parameter x increase the region of parameters where the cotransport is happening. All these observations clearly show that molecular mechanisms of antiporters are kinetically and not thermodynamically controlled, in contrast to current views in the field.

To understand better the microscopic picture of dynamic processes in antiporters, we might consider again eq 6 for the situation when all transition rates are fixed but the catalytic effect can be varied. It can be shown that there is a critical value of $x = x_c$,

$$x_c = \frac{\frac{w_A}{u_A'}(g_B - 1)}{(g_A - g_B) - \frac{2\gamma}{u_A'}(g_B - 1)} \tag{7}$$

such that for $x > x_c$ the antiporters are functioning normally and move molecules B against their gradient, while for $x < x_c$ both types of species follow their gradients and the antiporter is not functional. Since the conformational transition rate is typically slow, $\gamma/u_A' \ll 1$, this kinetic boundary can be well approximated for realistic conditions as

$$x_c \simeq \frac{\frac{w_A}{u_A'}(g_B - 1)}{(g_A - g_B)} \tag{8}$$

The physical meaning of this boundary is the following. If the concentration gradient of particles B is significant [large $(g_B - 1)$], then the system needs to have a stronger catalytic effect to overcome this barrier. Increasing the dissociation rate w_A has the same effect. It lowers the probability to find the system in the states 1 and 2 (see Figure 1), and to keep the same flux of particles A in order to drive the cotransport one needs to increase significantly the catalytic effect. However, increasing the difference between thermodynamic forces for the species A and B [large $(g_A - g_B)$] has the opposite effect. In this case, relatively weak catalytic effect is enough to drive the cotransport because the driving force to move the particles B is already strong.

It is interesting to note that, according to our calculations, the dissociation rate w_B does not play any role in kinetic conditions of the secondary active transport. We might explain this observation by analyzing the processes in Figure 1. It is clear that in order to make the antiporter operational one needs to have strong enough current of particles A, but the rate w_B does not affect much this flux. This might be the reason for the fact that kinetic conditions are independent of the dissociation rate w_B but at the same time changes in w_A are important.

To visualize the conditions that lead to antiporter functioning, it is convenient to analyze stationary probabilities for different chemical states as presented in Figure 3. One can see that for $x < x_c$, when the antiporter is not working, the probabilities for the system to be found in the states 2 and 3 are relatively small. In this case, we have transport of particles

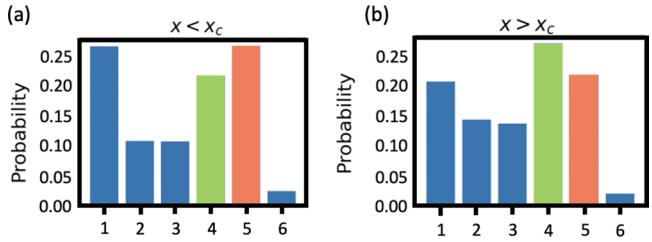

Figure 3. Stationary probabilities for different chemical states of the antiporter. (a) Regime when the transporter is not working; (b) regime when the cotransport is functional. The following parameters were used in calculations: $\gamma = 1\ s^{-1}$, $w_A = w_B = 100\ s^{-1}$, $u_A = 1000\ s^{-1}$, $u_B = 900\ s^{-1}$, $u_A' = 100\ s^{-1}$, $u_B' = 200\ s^{-1}$, and $x = 1$ in plot a and $x = 11$ in the plot b.

B along their concentration gradient ($P_5 > P_4$). The situation changes dramatically for $x > x_c$ when the cotransport is occurring. Here, the system increases the probabilities to be found in the states 2 and 3, and the occupation of states 4 and 5 reverses ($P_5 < P_4$). The increase in the population of the state 3 is important because it effectively pushes the flux of particles B to move against their thermodynamic force; see Figure 1.

The important function of antiporters is not only to force one of the substrates to move against its concentration gradient but also to keep the flux of such molecules high enough so that all necessary transportation tasks are accomplished on time. This is because the cellular dynamics is fast, and it also requires changes in concentrations of relevant molecules to happen fast. This suggests that kinetic parameters might be optimized for the efficient functioning of membrane transporters. Our theoretical approach can be conveniently utilized to analyze the degree of optimization in the cotransport. For this purpose, we explicitly evaluate both particle currents, $J_A = x\gamma(P_1 - P_2)$ and $J_B = x\gamma(P_4 - P_5)$, for different sets of kinetic parameters of the system. The results are presented in Figure 4.

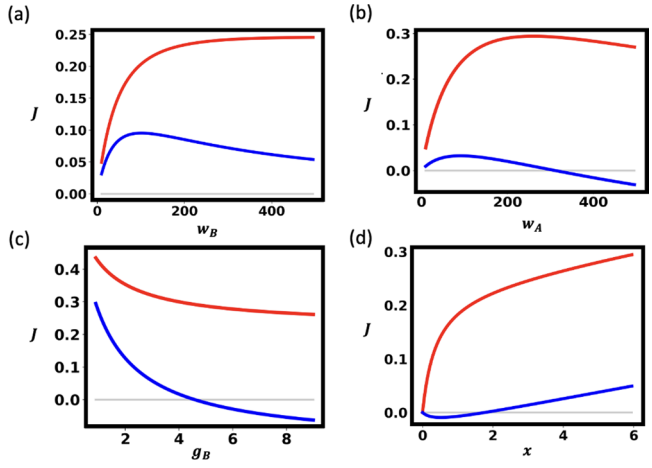

Figure 4. Particle fluxes of molecules A (red) and B (blue) as a function of (a) the dissociation rate w_B; (b) the dissociation rate w_A; (c) the thermodynamic force for the species B, expressed via g_B; and (d) the catalytic parameter x. Gray horizontal line corresponds to zero flux. The following parameters were used in calculations: (a) $\gamma = 1\ s^{-1}$, $w_A = w_B = 100\ s^{-1}$, $u_A = 1000\ s^{-1}$, $u_B = 900\ s^{-1}$, $u_A' = 100\ s^{-1}$, $u_B' = 200\ s^{-1}$, and $x = 2$; (b) the same parameters as for panel a but with $w_B = 1000\ s^{-1}$; (c) the same parameters as for panel a but with $w_A = 300\ s^{-1}$ and $w_B = 1000\ s^{-1}$; (d) the same parameters as for panel a but with $u_B' = 150\ s^{-1}$ and $w_B = 1000\ s^{-1}$.

https://doi.org/10.1021/acs.jpclett.1c02846
J. Phys. Chem. Lett. 2021, 12, 9588−9594

One can see that varying different kinetic parameters changes the fluxes of both substrates in antiporters in a complex way. Increasing the dissociation rate w_B has a different effect on J_A and J_B: see Figure 4a. It increases the particle flux of molecules A, while the change in the particle flux of molecules B is nonmonotonic. This can be understood by analyzing the molecular transitions shown in Figure 1. Larger values of w_B increase the relative fraction of the states 3 and 6, and this benefits the translocation of particles A by stimulating transitions in the direction $6 \rightarrow 1 \rightarrow 2 \rightarrow 3 \rightarrow 6$. At the same time, the change in the dissociation rate w_B has two opposite effects on the particle flux J_B. It accelerates the transition $5 \rightarrow 6$ (Figure 1), which should increase the flux of molecules B. But it also simultaneously accelerates the transition $4 \rightarrow 3$ (see Figure 1), which should lower the flux of molecules B. As a result of these two opposing processes, the flux J_B depends nonmonotonically on w_B.

Varying the dissociation rate w_A has a nonmonotonic effect of particle fluxes of both species: see Figure 4b. This is because increasing this dissociation rate pushes the flux of particles A in two different directions. From one side, it should increase J_A by accelerating the transition $2 \rightarrow 3$ (Figure 1), but from another side, it should lower J_A by accelerating the transition $1 \rightarrow 6$ (Figure 1). In other words, the particles A are mostly binding and unbinding to the channel instead of translocating. The consequence of this is also that for large w_A the flux of species B will also start to decrease. This happens due to the increase in the thermodynamic drive which correlates with the strength of the flux J_A.

The dependence of the particle fluxes on varying g_B (see Figure 4c) is expected. Keeping all parameters the same but increasing thermodynamic drive for species B lowers the overall thermodynamic force $(g_A - g_B)$ that drives the cotransport in this system. The weaker driving force decreases J_A, and because the translocations of both types of species are coupled in the transporter this also lowers J_B. Varying the catalytic parameter x has a similar effect on both currents for almost all values of x. This is because it accelerates transitions $1 \leftrightarrow 2$ and $4 \leftrightarrow 5$, allowing for better coupling in the system and increasing the cotransport effect.

The results presented in Figure 4 suggest that antiporters might increase the flux of particles B by tuning the specific kinetic parameters. But there is another angle of how the functioning of these membrane channels can be optimized. One could define a new parameter, $\eta = J_B/J_A$, that quantifies the efficiency of the antiporter. These transporters are very efficient when $\eta \approx 1$, while they are not efficient when $\eta \approx 0$. Again, our theoretical method can be conveniently used to investigate the efficiency.

Using eqs 2, one can derive that

$$\eta = \frac{J_B}{J_A} = \frac{P_5 - P_4}{P_1 - P_2} = \frac{u_B'(w_A + 2\gamma x + u_A x) - u_B(w_A + 2\gamma x + u_A' x)}{u_A(w_B + 2\gamma x + u_B' x) - u_A'(w_B + 2\gamma x + u_B x)} \quad (9)$$

which can expressed using the measures of thermodynamic forces g_A and g_B

$$\eta = \frac{\left[(g_A - g_B) - \frac{2\gamma}{u_A'}(g_B - 1)\right]x - \frac{w_A}{u_A'}(g_B - 1)}{\left[(g_A - g_B) + \frac{2\gamma}{u_B'}(g_A - 1)\right]x + \frac{w_B}{u_B'}(g_A - 1)} \quad (10)$$

Since the conformational transition rates for unoccupied channels in realistic antiporters are typically quite small ($\gamma/u_A' \ll 1$ and $\gamma/u_B' \ll 1$), the expression for the efficiency coefficient can be further approximated as

$$\eta \simeq \frac{(g_A - g_B)x - \frac{w_A}{u_A'}(g_B - 1)}{(g_A - g_B)x + \frac{w_B}{u_B'}(g_A - 1)} \quad (11)$$

It is interesting to evaluate the efficiency in several limiting situations. When the concentration gradient of species A is extremely high ($g_A \gg g_B > 1$) it can be shown from eq 11 that

$$\eta \simeq \frac{x}{x + \frac{w_B}{u_B'}} < 1 \quad (12)$$

This is a surprising result since in this case one could expect 100% efficiency for essentially infinite thermodynamic driving force. The same result is also obtained in another limit, $g_B = 1$. This result is again surprising because this case corresponds to zero thermodynamic resistance from species B where the highest efficiency is expected. These observations support our arguments that there are additional kinetic constraints in the system that lower the overall efficiency, but they must be overcome in order for the transporter to be functional.

One could also see from eqs 10 and 11 the importance of the catalytic effect. Increasing the parameter x always improves the efficiency of the antiporter system. But there is an additional advantage of having large catalytic effect, as illustrated in Figure 5. Here we present the efficiency as the function of the ratio g_B/g_A. The cellular environment is very dynamic and strong fluctuations in concentrations of substrates and other molecules that might affect the kinetic parameters of translocation (e.g., pH and ionic strength) are expected. Varying this ratio mimics the possibility of such fluctuations in the concentrations inside and the outside of the cell. One can see that for relatively weak catalytic effect (Figure 5a), the fluctuations will strongly affect the efficiency. It is quite sensitive to the variation in the ratio g_B/g_A. At the same time, for large x (Figure 5b) the efficiency of the transporter with respect to the fluctuations is quite robust. The coefficient η does not depend strongly on the ratio g_B/g_A for a large range of parameters. These observations suggest that the large catalytic effect not only allows the particle fluxes of two substrates to be coupled better to support the operation of antiporters, but it

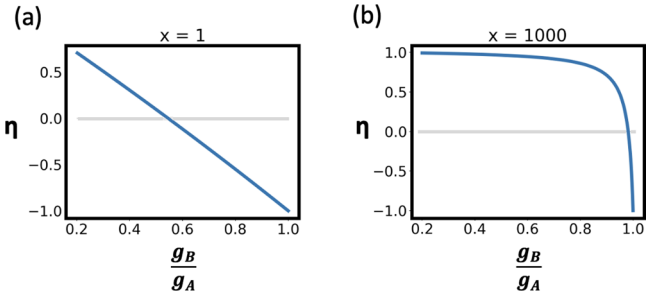

Figure 5. Efficiency of an antiporter as a function of the ratio of the concentration gradient of compound B to the concentration gradient of compound A when (a) $x = 1$ and (b) $x = 1000$. Gray horizontal line corresponds to zero efficiency. The following parameters were used in calculations: $\gamma = 1\ s^{-1}$, $w_A = w_B = 100\ s^{-1}$, $u_A = 1000\ s^{-1}$, $u_B = 1000\ s^{-1}$, $u_A' = 100\ s^{-1}$, $u_B' = 200\ s^{-1}$.

https://doi.org/10.1021/acs.jpclett.1c02846
J. Phys. Chem. Lett. 2021, 12, 9588−9594

also makes these membrane channels very efficient and robust translocation machines.

Our theoretical findings naturally explain the existence of a large number of transporters with similar structures in the same biological cells. We suggest that this is a result of optimizations that better reflect the fluctuations in local concentrations of substrates and other kinetic parameters. For example, variations in pH in channels that do not use the transport of protons might influence the dissociation rates of substrates. This will clearly modify the kinetic constraints, and it is possible that nature developed different antiporters to be efficient and robust in this highly dynamic cellular environment.

In this Letter, we presented a theoretical investigation of molecular mechanisms of secondary active transport in antiporters that use the concentration gradient of one type of substrate to translocate the other type of substrate against its concentration gradient. We specifically analyzed a minimal chemical-kinetic model that takes into account the most relevant states and considers all chemical transitions in a thermodynamically consistent way. This allowed us to obtain full analytical solutions of dynamic properties of the system at steady-state conditions. Our analysis suggests that antiporters are governed by kinetic conditions and not the thermodynamic conditions, as was previously assumed. For any fixed set of thermodynamic forces in the system, there is additional energy that need to be spent in order to overcome the kinetic constraints. This is our main result, which is obtained by thermodynamically consistent analysis of the underlying chemical-kinetic model of antiporters. In addition, we show that the translocating particle fluxes can be optimized by tuning some kinetic parameters. Furthermore, our theoretical approach proposes how to evaluate the efficiency of the antiporter. We also discuss multiple roles of the catalytic effect, when the binding of substrates accelerates the conformational transitions in the system, in making transportation via membrane channels more efficient and fast. It is also argued that our theoretical picture might explain a wide spectrum of existing antiporters for the same transportation tasks.

Although the presented theoretical study provides a simple, physically clear, and fully quantitative approach to clarify the microscopic picture of cotransport, it is important to discuss its limitations and possible extensions. In our model, catalytic acceleration effects are taken to be the same for both types of particles, but it is more realistic to expect them to be different. In addition, we assumed that dissociation rates of substrates are the same for the channels opened up and opened down, which might not be the case. Furthermore, following the common views in the field, our model considers only the catalytic effect of substrates after binding to the channel. This corresponds to changing only the conformational energy barriers but not the free energy difference between the corresponding channel states. It might be interesting to explore more this energetic point of view for the translocation processes in antiporters. Another interesting direction of future studies is to understand the molecular mechanisms of symporters where both fluxes move in the same direction. The question here is if one can still use the single-site model similar to what we explored for antiporters or the symmetry would require more sophisticated multisite approaches. It will be important to test our theoretical predictions in more advanced theoretical and experimental studies.

AUTHOR INFORMATION

Corresponding Author

Anatoly B. Kolomeisky − *Department of Chemistry, Center for Theoretical Biological Physics, Department of Chemical and Biomolecular Engineering, and Department of Physics and Astronomy, Rice University, Houston, Texas 77005, United States;* orcid.org/0000-0001-5677-6690; Email: tolya@rice.edu

Author

Alex Berlaga − *Department of Chemistry, Rice University, Houston, Texas 77005, United States*

Complete contact information is available at: https://pubs.acs.org/10.1021/acs.jpclett.1c02846

Notes

The authors declare no competing financial interest.

ACKNOWLEDGMENTS

This work was supported by the Welch Foundation (C-1559), by the NSF (CHE-1953453 and MCB-1941106), and by the Center for Theoretical Biological Physics sponsored by the NSF (PHY-2019745).

REFERENCES

(1) Lodish, H.; Zipursky, S. L. *Molecular cell biology*; W. H. Freeman: New York, 2001; Vol. *29*, pp 580−602.

(2) Alberts, B.; Johnson, A.; Lewis, J.; Morgan, D.; Raff, M.; Roberts, K.; Walter, P. *Molecular Biology of the Cell*, 6th ed; Garland Science: New York, NY, 2014.

(3) Law, C. J.; Maloney, P. C.; Wang, D.-N. Ins and Outs of Major Facilitator Superfamily Antiporters. *Annu. Rev. Microbiol.* **2008**, *62*, 289−305.

(4) Mueckler, M.; Thorens, B. The SLC2 (GLUT) family of membrane transporters. *Mol. Aspects Med.* **2013**, *34*, 121−138.

(5) Blaesse, P.; Airaksinen, M. S.; Rivera, C.; Kaila, K. Cation-Chloride Cotransporters and Neuronal Function. *Neuron* **2009**, *61*, 820−838.

(6) Stillwell, W. Membrane transport. *An introduction to biological membranes: from bilayers to rafts*; Elsevier, 2013; p 305.

(7) Yang, N. J.; Hinner, M. J. Getting across the cell membrane: an overview for small molecules, peptides, and proteins. *Methods Mol. Biol.* **2015**, *1266*, 29−53.

(8) Drew, D.; Boudker, O. Shared molecular mechanisms of membrane transporters. *Annu. Rev. Biochem.* **2016**, *85*, 543−572.

(9) Poulsen, S. B.; Fenton, R. A.; Rieg, T. Sodium-glucose cotransport. *Curr. Opin. Nephrol. Hypertens.* **2015**, *24*, 463.

(10) Darrouzet, E.; Lindenthal, S.; Marcellin, D.; Pellequer, J.-L.; Pourcher, T. The sodium/iodide symporter: state of the art of its molecular characterization. *Biochim. Biophys. Acta, Biomembr.* **2014**, *1838*, 244−253.

(11) LeVine, M. V.; Cuendet, M. A.; Khelashvili, G.; Weinstein, H. Allosteric mechanisms of molecular machines at the membrane: transport by sodium-coupled symporters. *Chem. Rev.* **2016**, *116*, 6552−6587.

(12) Navratna, V.; Gouaux, E. Insights into the mechanism and pharmacology of neurotransmitter sodium symporters. *Curr. Opin. Struct. Biol.* **2019**, *54*, 161−170.

(13) Ito, M.; Morino, M.; Krulwich, T. A. Mrp antiporters have important roles in diverse bacteria and archaea. *Front. Microbiol.* **2017**, *8*, 2325.

(14) Padan, E.; Venturi, M.; Gerchman, Y.; Dover, N. Na+/H+ antiporters. *Biochim. Biophys. Acta, Bioenerg.* **2001**, *1505*, 144−157.

(15) Forrest, L. R.; Rudnick, G. The Rocking Bundle: A Mechanism for Ion-Coupled Solute Flux by Symmetrical Transporters. *Physiology* **2009**, *24*, 377−386.

(16) Mayes, H. B.; Lee, S.; White, A. D.; Voth, G. A.; Swanson, J. M. Multiscale kinetic modeling reveals an ensemble of Cl−/H+ exchange pathways in ClC-ec1 antiporter. *J. Am. Chem. Soc.* **2018**, *140*, 1793−1804.
(17) Paulino, C.; Wöhlert, D.; Kapotova, E.; Yildiz, Ö.; Kühlbrandt, W. Structure and transport mechanism of the sodium/proton antiporter MjNhaP1. *eLife* **2014**, *3*, e03583.
(18) Law, C. J.; Yang, Q.; Soudant, C.; Maloney, P. C.; Wang, D.-N. Kinetic evidence is consistent with the rocker-switch mechanism of membrane transport by GlpT. *Biochemistry* **2007**, *46*, 12190−12197.
(19) Pradhan, R. K.; Beard, D. A.; Dash, R. K. A biophysically based mathematical model for the kinetics of mitochondrial Na+-Ca2+ antiporter. *Biophys. J.* **2010**, *98*, 218−230.
(20) Hill, T. L. *Free energy transduction and biochemical cycle kinetics*; Courier Corporation, 2005.
(21) Berezhkovskii, A. M.; Lizunov, V. A.; Zimmerberg, J.; Bezrukov, S. M. Functional Role for Transporter Isoforms in Optimizing Membrane Transport. *Biophys. J.* **2011**, *101*, L14−L16.
(22) Krupka, R. Role of substrate binding forces in exchange-only transport systems: II. Implications for the mechanism of the anion exchanger of red cells. *J. Membr. Biol.* **1989**, *109*, 159−171.
(23) Krupka, R. Role of substrate binding forces in exchange-only transport systems: I. Transition-state theory. *J. Membr. Biol.* **1989**, *109*, 151−158.

https://doi.org/10.1021/acs.jpclett.1c02846
J. Phys. Chem. Lett. 2021, 12, 9588−9594